

# Development of a Parallel Reaction Monitoring Mass Spectrometry Assay for the Detection of SARS-CoV-2 Spike Glycoprotein and Nucleoprotein

Lisa H. Cazares, Raghothama Chaerkady, Shao Huan Samuel Weng, Chelsea C. Boo, Raffaello Cimbri, Hsiang-En Hsu, Sarav Rajan, William Dall'Acqua, Lori Clarke, Kuishu Ren, Patrick McTamney, Nicole Kallewaard-LeLay, Mahboobe Ghaedi, Yasuhiro Ikeda, and Sonja Hess\*



Cite This: <https://dx.doi.org/10.1021/acs.analchem.0c02288>



Read Online

ACCESS |



Metrics & More

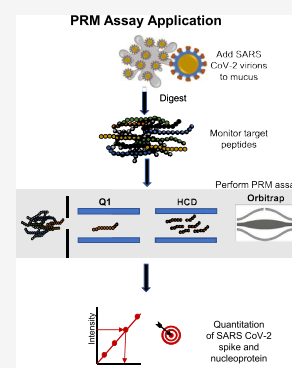


Article Recommendations



Supporting Information

**ABSTRACT:** There is an urgent need for robust and high-throughput methods for SARS-CoV-2 detection in suspected patient samples to facilitate disease management, surveillance, and control. Although nucleic acid detection methods such as reverse transcription polymerase chain reaction (RT-PCR) are the gold standard, during the current pandemic, the deployment of RT-PCR tests has been extremely slow, and key reagents such as PCR primers and RNA extraction kits are at critical shortages. Rapid point-of-care viral antigen detection methods have been previously employed for the diagnosis of respiratory viruses such as influenza and respiratory syncytial viruses. Therefore, the direct detection of SARS-CoV-2 viral antigens in patient samples could also be used for diagnosis of active infection, and alternative methodologies for specific and sensitive viral protein detection should be explored. Targeted mass spectrometry techniques have enabled the identification and quantitation of a defined subset of proteins/peptides at single amino acid resolution with attomole level sensitivity and high reproducibility. Herein, we report a targeted mass spectrometry assay for the detection of SARS-CoV-2 spike protein and nucleoprotein in a relevant biological matrix. Recombinant full-length spike protein and nucleoprotein were digested and proteotypic peptides were selected for parallel reaction monitoring (PRM) quantitation using a high-resolution Orbitrap instrument. A spectral library, which contained seven proteotypic peptides (four from spike protein and three from nucleoprotein) and the top three to four transitions, was generated and evaluated. From the original spectral library, we selected two best performing peptides for the final PRM assay. The assay was evaluated using mock test samples containing inactivated SARS-CoV-2 virions, added to *in vitro* derived mucus. The PRM assay provided a limit of detection of  $\sim 200$  attomoles and a limit of quantitation of  $\sim 390$  attomoles. Extrapolating from the test samples, the projected titer of virus particles necessary for the detection of SARS-CoV-2 spike and nucleoprotein detection was approximately  $2 \times 10^5$  viral particles/mL, making it an attractive alternative to RT-PCR assays. Potentially, mass spectrometry-based methods for viral antigen detection may deliver higher throughput and could serve as a complementary diagnostic tool to RT-PCR. Furthermore, this assay could be used to evaluate the presence of SARS-CoV-2 in archived or recently collected biological fluids, *in vitro*-derived research materials, and wastewater samples.



Sensitive, specific, and rapid diagnostic tests are needed for the detection of pathogens such as SARS-CoV-2, which is responsible for the pandemic outbreak, which began in December 2019 in Wuhan, China. So far, nucleic acid tests and antibody detection assays have been employed for the diagnosis for SARS-CoV-2 infection (Figure 1). SARS-CoV-2 reverse transcription polymerase chain reaction (RT-PCR) diagnostic assays preferentially target the S and nucleocapsid (N) genes, the nonstructural RNA-dependent RNA polymerase and replicase open reading frame 1a/b genes.<sup>1</sup> In SARS-CoV-2 virus-infected patients, the most reliable samples for detection via RT-PCR are nasal and pharyngeal swabs, and sputum/mucus, but not blood samples.<sup>2,3</sup> Indeed, in one study, only 15% of patients hospitalized with SARS-CoV-2-induced pneumonia had detectable RNA in serum.<sup>3</sup> While principally satisfying the requirements for rapid sensitive, specific, and

rapid diagnostic tests, the deployment of RT-PCR tests has been extremely slow, especially in the U.S. and parts of Europe, and key reagents such as PCR primers and RNA extraction kits are at critical shortages to enable wide-screen testing of the general public, requiring hundreds of millions, if not billions of tests in a very short period of time. As alternatives to the detection of the viral genome through molecular amplification, serological tests, which detect antibodies to SARS CoV-2 in

Received: May 28, 2020

Accepted: September 23, 2020

Published: September 23, 2020

	Direct Detection		Indirect Detection
Analyte	Virus RNA	Virus Antigen	Antibodies specific to SARS CoV-2
Detection method	RT-PCR	Immuno-ELISA Mass Spectrometry	ELISA or lateral flow
Specificity	+++	++ +++	++

**Figure 1.** Methods employed for the detection of SARS CoV-2 viral infection. Direct detection methods such as RT-PCR which detects viral RNA are the most specific and widely employed for the diagnosis of SARS CoV-2 infection. Other direct detection methods that look for the presence of viral antigen are performed using an immunoassay/ELISA. Methods which employ mass spectrometry for antigen detection can offer a higher level of specificity and potentially sensitivity. Indirect methods are used for the detection of antibodies to SARS CoV-2 and can be performed using immunoassays such as ELISA or lateral flow. These methods can only report if an individual has been exposed to the virus and not if they are currently infected and shedding virus.

blood samples, have been developed. Unlike RT-PCR tests, immunoassays that target immunoglobulin M and G (IgM, IgG) host responses are less susceptible to sequence erosion due to genetic drift. Knowledge of individuals who have been previously infected with SARS-CoV-2 and have produced antibodies would be crucial information to guide necessary quarantine strategies and determine accurate mortality rates. However, because of the delay of antibodies generated in SARS-CoV-2-infected humans, serological testing for antibodies will not be of use to prevent disease spread during an outbreak.<sup>4</sup> Rapid point-of-care viral antigen detection methods have been employed previously for the diagnosis of respiratory viruses such as influenza and respiratory syncytial viruses,<sup>5</sup> and have most recently been developed for coronaviruses, but are plagued by the lack of specificity and sensitivity.

The spike glycoprotein (S) on the surface of SARS-CoV-2, which is a major antigenic target,<sup>6</sup> and the nucleoprotein (NP), which packages the viral RNA can be exploited by specific, targeted mass spectrometry (MS) assays. Continuously improving targeted MS instruments and methodologies have enabled the identification and quantitation of a defined subset of proteins/peptides at single amino acid resolution with attomole level sensitivity and high reproducibility.<sup>7,8</sup> This approach has the potential to quantitate over 1000 proteins in a single analysis, including isoforms, and is, therefore, far superior in terms of specificity and multiplexing capability to conventional protein measurement methods, which rely on immunoaffinity [i.e., enzyme-linked immunosorbent assay (ELISA)]. Furthermore, the extendibility of targeted proteomic MS assays to the analysis of newly discovered proteins can be accomplished in a convenient and extremely time-efficient manner. For this reason, targeted MS is gaining popularity as a promising clinical diagnostic tool in a wide variety of disease conditions such as cancer<sup>9,10</sup> and cardiovascular disease<sup>11</sup> and can also be used to monitor the levels of proteins that are targets of therapeutic treatment.<sup>12</sup> While preliminary studies have indicated feasibility,<sup>13,14</sup> the potential for the application of targeted MS has not been fully explored for infectious disease diagnostics.

To determine the feasibility of targeted MS for SARS-CoV-2 diagnostics, we developed a method for the detection and quantitation of the S and NP, which employs parallel reaction monitoring (PRM) using a high-resolution Orbitrap instrument, thereby providing very high specificity. This method,

which monitors 2 proteotypic peptides, exhibited a limit of detection (LOD) of  $\sim 200$  amol and a limit of quantitation (LOQ) of  $\sim 390$  amol. To test the ability of the PRM assay to detect S protein and NP in a relevant sample type, we spiked inactivated SARS CoV-2 virions into in vitro derived mucus. Using this mock sample, the projected titer of virus particles necessary for the detection of SARS-CoV-2 S-protein detection was  $\sim 2 \times 10^5$  pfu/mL, making it an attractive alternative to RT-PCR assays.

## MATERIALS AND METHODS

**Chemicals and Reagents.** Sodium dodecyl sulfate (SDS), ultrapure, was purchased from (J.T. Baker). Triethylammonium bicarbonate (TEAB) 1 M, ammonium bicarbonate, and *ortho*-phosphoric acid 85% were purchased from Sigma. Tris(2-carboxyethyl)phosphine (TCEP) and iodoacetamide  $\geq 98\%$ , Proteomics Grade, were purchased from VWR. Acetonitrile and methanol (LC-MS grade) were purchased from Fisher Scientific. Formic acid was obtained from Merck. Heavy labeled peptides for S and NP proteins were obtained from 21st Century Biochemicals, Inc. Amino acid purity was  $>99\%$  and the peptide content was corrected based on the amino acid analysis data provided by the vendor.

**Full-Length SARS-CoV-2 Spike Protein and NP.** SARS-CoV-2 prefusion S ectodomain protein (residues 1–1208) was generated as previously described.<sup>15</sup> SARS-CoV-2 receptor binding domain (RBD) (residues 334–526) (GenBank: MN908947) was cloned with an N-terminal CD33 leader sequence and a C-terminal GSSG linker, AviTag (GLNDI-FEAQKIEWHE), GSSG linker, and 8 $\times$  HisTag, while SARS-CoV-2 N-terminal domain (NTD) (residues 16–305) was cloned with an N-terminal CD33 leader sequence and a C-terminal GSSG linker and 8 $\times$  HisTag. Full-length spike proteins were expressed in FreeStyle 293 cells (Thermo Fisher) and isolated by affinity chromatography using HisTrap columns (GE Healthcare) followed by size exclusion chromatography with a Superdex 200 column (GE Healthcare). Purified proteins were analyzed by sodium dodecyl sulfate polyacrylamide gel electrophoresis to ensure purity and appropriate molecular weights. SARS-CoV-2 nucleocapsid-His recombinant protein was purchased from Sino Biological (100  $\mu$ g, 40588-V08B) The protein was difficult to dissolve and required treatment before S-trap preparation below with 40  $\mu$ L dimethyl sulfoxide (276855–100 mL, Sigma), 126  $\mu$ L 1%

TFA, and 100  $\mu\text{L}$  1 $\times$  S-Trap lysis buffer (5% SDS, 50 mM TEAB, pH adjusted to 7.55 using 12% phosphoric acid).

**SARS-CoV-2 Virus Stock.** SARS-CoV-2 inactivated virus was kindly provided by the NIAID Integrated Research Facility (Frederick, Maryland). Briefly, Grivet (*Chlorocebus aethiops*) kidney epithelial cells (ATCC catalog# CCL-81) were infected with SARS-CoV-2 (USA\_WA1/2020:IRF399) at an MOI of 0.01. Cells were incubated for 48 h at 37  $^{\circ}\text{C}$  in 5%  $\text{CO}_2$ . Culture supernatant was collected and combined with 0.25 volumes of 4 $\times$  NuPAGE LDS sample buffer (Life Technologies Cat# NP0007) and 10 $\times$  NuPAGE Reducing Agent (Cat# NP0004) to a 1 $\times$  final mixture. Samples were then heated to 95  $^{\circ}\text{C}$  for 10 min to complete virus inactivation. The titer of the virus stock was approximately  $9.26 \times 10^6$  PFU/mL, accounting for its dilution in inactivation buffer.

**S-Trap Digestion.** SARS-CoV-2 full-length S-protein (392 ng) in PBS and cultured lung epithelial cell mucus secretions (40  $\mu\text{g}$ ) were denatured at 65  $^{\circ}\text{C}$  for 45 min using equal volumes of 2 $\times$  S-Trap lysis buffer (10% SDS, 100 mM TEAB, pH adjusted to 7.55 using 12% phosphoric acid) and 10 mM TCEP (200 mM TCEP in 770 mM TEAB, pH 7.8).<sup>16</sup> Reduced proteins were then alkylated with 40 mM iodoacetamide in the dark for 30 min at room temperature. Samples were acidified using 12% phosphoric acid (final concentration 1.2%) and diluted using 6 $\times$  volume of S-Trap binding buffer (methanol containing 100 mM TEAB, pH adjusted to 7.2 using 12% phosphoric acid). Diluted sample nucleocapsid recombinant protein (126 ng) was loaded 100  $\mu\text{L}$  at a time onto an S-Trap micro column using a microcentrifuge (Sonation Devices) with a flow-through a waste collector. Finally, SDS was completely removed from the sample by washing the filter four times with 160  $\mu\text{L}$  of S-Trap binding buffer. Pure protein samples on the filter were then digested using 2  $\mu\text{g}$  of trypsin/Lys-C (#V5073, Promega) in 50 mM ammonium bicarbonate, 0.5 mM  $\text{CaCl}_2$  at 47  $^{\circ}\text{C}$  for 2 h. Digested peptides were collected by washing the filter in three steps with 40  $\mu\text{L}$  of 50 mM ammonium bicarbonate, 40  $\mu\text{L}$  of 0.1% formic acid, and 35  $\mu\text{L}$  of 0.1% formic acid in 50% acetonitrile. Eluate was dried in vacuo and stored at  $-80$   $^{\circ}\text{C}$  prior to analysis. Additional chymotrypsin digestion (1:20) was carried out for the tryptic peptides to characterize glycosylation sites.

**Generation of In vitro Derived Mucus.** Human airway basal cells (BCs) were isolated from distal tracheas of normal lungs obtained from donors. BCs at passage 1–2 were seeded on a 0.4  $\mu\text{M}$  polyester porous membrane insert and were differentiated for 3 weeks at the air-liquid interface. For mucin collection, 200  $\mu\text{L}$  of PBS was added to the apical surface and incubated for 30 min at 37  $^{\circ}\text{C}$ . PBS/mucin was then removed with a pipette and stored at  $-80$   $^{\circ}\text{C}$  for later use in the PRM assay.

**Preparation of Dilution Series Using Full-Length S-Protein and NP.** A 2-fold dilution series over a  $10^6$  dynamic range was generated as previously described,<sup>17</sup> which contained SARS-CoV-2 S and NP peptides in a range of 3 amol to 12.5 fmol in 0.4  $\mu\text{g}$  in vitro derived mucus digest containing 12.5 fmol of each synthetic heavy peptide (21st Century Biochemicals, Inc., USA, MA), and 62.5 fmol of indexed retention time standard (iRT peptides, Biognosys Boston, MA).<sup>18</sup> A “reverse” calibration curve was also constructed to evaluate quantification accuracy in which the concentration of the isotopically labeled peptides was varied from 3 amol to 25 fmol, while the light peptide concentration

remained fixed at 12.5 fmol. Two-fold dilution was performed in triplicate for each concentration. Based on the slope and y-intercept from the two calibration curves in the linear regression analysis, the corresponding concentration for each point was calculated. The correlation between the two calibrations was evaluated where close to 1 indicates the value between the two calibration curves is well correlated.

**Preparation of SARS-CoV-2 Virus-Spiked Mucus Samples.** Two different amounts of SARS-CoV-2 viral particles representing: 3.125  $\mu\text{L}$  (low) and 12.5  $\mu\text{L}$  (high) amounts of an inactivated stock solution were spiked into 16  $\mu\text{g}$  of cultured lung epithelial cell mucus secretions. A negative control mucus sample was also run, which contained no virus. The sample was then subjected to the S-Trap digestion protocol described above in a total starting volume of 150  $\mu\text{L}$ . Indexed retention time (iRT) peptides (62.5 fmol) were spiked into the digested samples prior to the nLC-MS/MS analysis.

**MS Methods.** Data-dependent acquisition (DDA) and PRM analyses were carried out on a Q-Exactive HF-X mass spectrometer interfaced with a Dionex Ultimate 3000 RSLCnano liquid chromatography system (Thermo Fisher Scientific). Samples were separated on a monolithic column (50 cm, cut from a 2 m long column, 100  $\mu\text{m}$  ID, GL Sciences Inc. USA) and coupled with a trap column (2 cm, 75  $\mu\text{m}$  ID, ReproSil-Pur 120 C18-AQ, 7  $\mu\text{m}$  Dr. Maisch GmbH) using a gradient of solvent A (0.2% formic acid) and solvent B (0.2% formic acid in 90% acetonitrile) as described below.

**DDA Analysis.** Samples (2–5  $\mu\text{L}$  containing 500 ng) were loaded onto a trap column with a flow rate of 6  $\mu\text{L}/\text{min}$  with solvent A for 2.5 min. The peptides were separated using a 55 min gradient of solvent B as follows: 2–8% B in 1.5 min, 8–28% B in 41 min, 28–45% B in 7 min, 45–70% B in 2 min, and 70–98% B for 3 min at a flow rate of 1.1  $\mu\text{L}/\text{min}$ . Peptides were sprayed in an electrospray ionization source using a stainless steel emitter with 2 kV at a capillary temperature of 275  $^{\circ}\text{C}$ . A full-scan MS spectrum was collected at 60,000 resolution at  $m/z$  of 200 and scanned at 365–1800  $m/z$  with automatic gain control (AGC) of  $3 \times 10^6$ . The top 12 precursors were selected, and MS/MS scan was obtained at 7500 resolution with a 50 ms injection time, an isolation window of 1.4  $m/z$ , and a normalized collision energy (NCE) of 28. For MS<sup>2</sup>, the AGC target was set to  $1 \times 10^5$  and the minimum AGC target was set to  $1 \times 10^4$ , which corresponds to an intensity threshold of  $2 \times 10^5$  per second. Dynamic exclusion duration was set to 20 s. The fixed first mass was set to 110  $m/z$ . Charge state exclusion was set to ignore unassigned, 1, and 7 and greater charges. For internal mass calibration, lock mass of 371.10124  $m/z$  ion was used.

**PRM Analysis.** For PRM, samples (1–2  $\mu\text{L}$ ) were run using a 7 min separation gradient with the following parameters: 4–12% B in 0.25 min, 12–30% B in 6.25 min, 30–45% B in 2.25 min, 45–98% B in 0.2 min, 98% B for 4 min, and 2% B for 2 min at a flow rate of 1.1  $\mu\text{L}/\text{min}$ . PRM data were acquired at 7500 resolution at  $m/z$  of 200 with an AGC of  $1 \times 10^5$  and a 100 ms ion injection time. Isolation list containing 28  $m/z$  targets from SARS-COV-2, mucin 5B, mucin 5AC, and iRT peptides was imported from Skyline (see Tables S2 and S3). The isolation window was set to 1.6  $m/z$ . NCE was set to 28 and the fixed first mass was set to 110  $m/z$ . Isotope-labeled peptide and endogenous peptide pairs were multiplexed together (MSX = 2) with the same injection time (isochronous injection times on mode).<sup>19,20</sup>

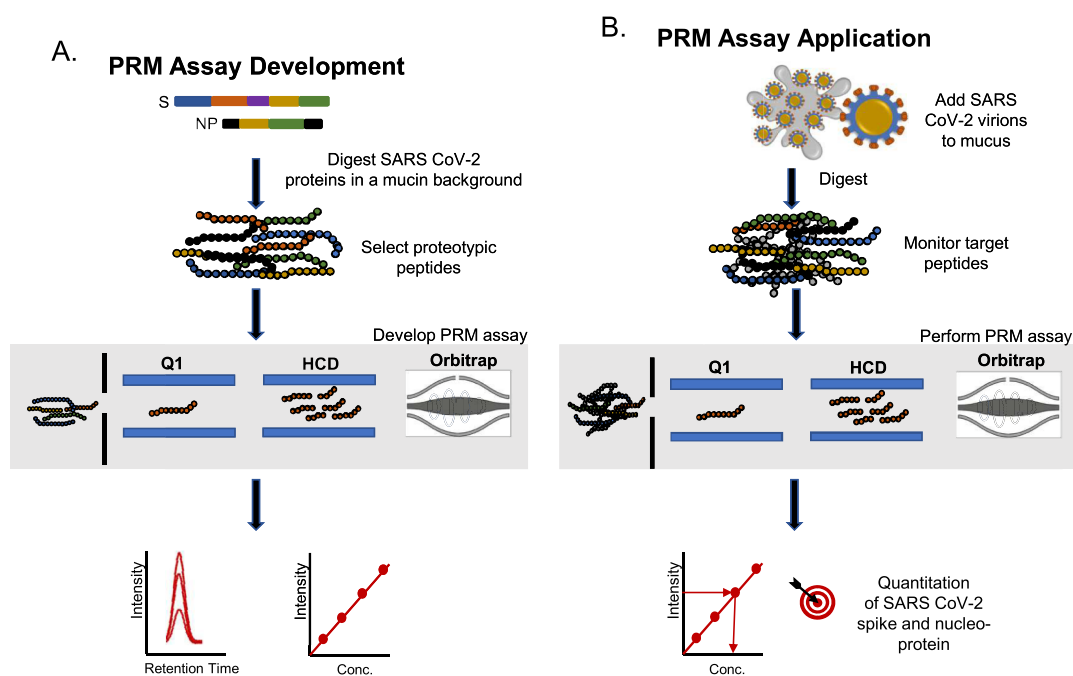


**Figure 2.** Schematic of the workflow used to develop a PRM assay for the detection and quantitation of SARS-CoV-2 spike and NP (A) PRM assay development was performed using recombinant SARS CoV-2 spike protein and NP. Proteotypic target peptides/transitions were selected to generate a spectral library in Skyline. (B) PRM assay was then used to quantitate the SARS-CoV-2 protein levels in a mock sample that was created by adding an inactivated virus sample to in vitro derived mucus.

**Data Analysis and PRM Assay Development.** Tandem mass spectrometry data of the Lys-C/trypsin digested samples were analyzed using a Proteome Discoverer (Thermo Fisher Scientific, ver. 2.4) interfaced with a Byonic search engine (ver. 3.7) with SARS-CoV-2 (Sequence ID\_6VSB, NCBI) and human Uniprot database 2019 including common contaminants. Targeted decoy peptide spectrum validator was set to 0.01 FDR. Isotope labels for arginine ( $^{13}\text{C}_6^{15}\text{N}_4$ ) and lysine ( $^{13}\text{C}_6^{15}\text{N}_2$ ) were included as C-terminal modifications.

Skyline software (ver. 20.1, MacCoss Lab Software) was used for PRM assay development of Lys-C/trypsin digested samples and analysis including peptide selection and heavy/light peptide ratio quantification. The SARS-CoV-2 and iRT spectral library were constructed using Proteome Discoverer searched files. Skyline peptide settings included 7–40 amino acids and iRT-based retention time prediction was enabled. Four transitions per peptides were selected based on the spectral library rank and dotp value greater than 0.95. The proteotypic peptides were verified using a peptide uniqueness checker in neXtprot.<sup>21</sup> Transition reports contained the peptide sequence, selected transitions, MS<sup>2</sup> selected peak areas, and a heavy/light ratio, which were generated from Skyline for further data analysis.

**Quantitation Analysis.** Light to heavy peptide ratios were used for the quantitation analysis. Data from the dilution series were evaluated by linear regression analysis using triplicates for each dilution point. The LOD was defined as the lowest concentration at which the peak for the analyte is detected with an S/N ratio of 3 and the mean result of the lowest standard is 3 SD above the blank results. LOQ was established as the lowest concentration that met the criteria of precision (CV  $\leq$  25%) and accuracy (RE  $\leq$  25%).<sup>22,23</sup> The estimation of the concentration in the mock clinical samples (one negative control and two viral spiked samples) was calculated based on the slope and y-intercept from the best fit line in the regression

analysis. To evaluate the intra- and interassay variations for each peptide in the calibration curve and mock virus sample data, triplicates of the SARS-CoV-2 spiked and nucleocapsid protein mixtures were prepared on two different days, whereas triplicates of the mock virus sample were prepared on three different days. Intra-assay CV was defined as the mean CV from the experiments on the same day. The interassay CV was calculated by two different methods: (1) replicate-based comparison; replicate 1 was compared across different days, replicate 2 was compared across different days, etc.; (2) mean CV (%) from the intra-assay across the different days. To analyze the missed cleavage level, we searched the DDA data including five missed cleavages in Proteome Discoverer interfaced with Byonic software. Percentage intensity area for the target peptide was compared with different missed cleavage forms.

## RESULTS AND DISCUSSION

**Selection of Tryptic Peptides for PRM Assay.** A schematic of the workflow used to develop a PRM assay for SARS-CoV-2 S and NP is shown in Figures 2 and S1. As with all targeted MS approaches, proteotypic peptides unique for the selected protein targets are needed for quantitation.<sup>9,17</sup> Ideally, target peptides (usually 5–25 amino acids) should be unique for the SARS-CoV-2 proteins and selected from different regions of a protein of interest. A recombinant SARS-CoV-2 S-protein monomer was produced using HEK93 cells in-house and a recombinant NP was purchased. To select optimal candidate peptides for PRM quantitation, the proteins were digested with Lys-C/trypsin, and the resulting peptides were analyzed using nLC-MS/MS on an Orbitrap instrument (Q Exactive HF-X Hybrid) using DDA. For the S-protein, peptides covering 84% of the protein were detected, and 17 glycosylation sites were characterized. A second digestion test was performed with trypsin and chymotrypsin to enhance the

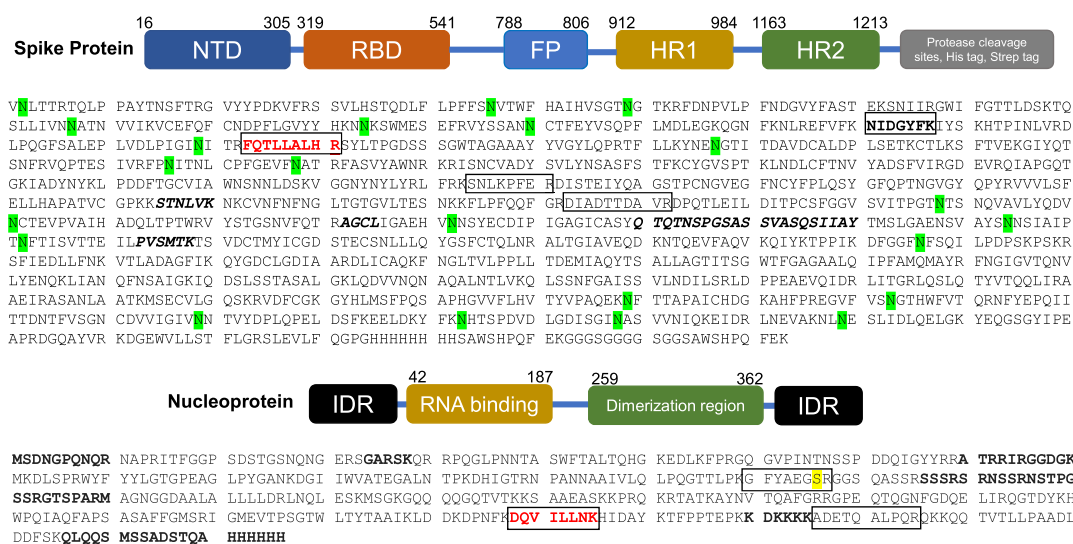


**Figure 3.** Sequence coverage and proteotypic target peptide selection for development of a PRM assay for the SARS CoV-2 Spike protein and NP. (Top panel) Diagram of SARS CoV-2 recombinant spike glycoprotein showing the location of NTD, RBD, fusion peptide and heptad repeats 1 and 2, and the protease cleavage sites, His and Strep tags. The amino acid sequence is given below. Glycosylation sites are indicated in green. (Bottom panel) Diagram of SARS CoV-2 recombinant NP showing intrinsically disordered regions, RNA binding and dimerization regions. Phosphorylation sites (S) are indicated in yellow. Bold italics indicate sites where sequence coverage was not obtained. Peptides monitored in the spectral library are boxed, peptides selected for the final PRM assay are boxed and indicated in red text. Overall 97.1% of the spike protein and 77.2% of the NP sequence was obtained from the DDA analysis.

**Table 1.** Peptides Selected for the SARS-COV-2 PRM Assay

peptide sequence	target	native (light) precursor $m/z$	charge state	aa sequence location	productions	$r^2$	% missed cleavages <sup>a</sup>	LOD <sup>b</sup> (attomoles)	LOQ <sup>b</sup> (attomoles)
DQVILLNK	NP	471.7846	2	348–355	$y^{2+}, y^{3+}, y^{4+}, y^{5+}$	0.9945	8.4	195	390
ADETQALPQR	NP	564.7858	2	376–385	$y^{3+}, y^{5+}, y^{6+}$	0.9931	29.5	195	390
NIDGYFK	S	428.7136	2	196–202	$y^{2+}, y^{3+}, y^{4+}, y^{5+}$	0.9833	18.9	195	390
FQTLALHR	S	366.8855	3	238–246	$y^{2+}, y^{3+}, y^{4+}, y^{5+}$	0.9863	0.21	195	390

<sup>a</sup>Determined from the sum of peptide intensity. <sup>b</sup>On column.

depth of sequence coverage and detection of glycosylation sites across the molecule. After identical nLC-MS/MS analysis, 97.1% sequence coverage was achieved, and five additional glycosylation sites were confirmed (Figure 3). Therefore, our data validated a previous report of 22 total glycosylation sites present on the native trimeric SARS-CoV-2 Spike protein.<sup>24</sup> This coverage was achieved only after performing an analysis capable of identifying large nontryptic glycosylated peptides (Byonic). For NP, after Lys-C/trypsin digestion, 77.2% coverage was achieved and one phosphorylation site was identified (S176), which has been previously reported.<sup>25</sup>

Based on this extensive sequence coverage and peptide response, we developed a list of tryptic peptide targets for subsequent PRM analysis, and obtained isotopically labeled standards for each peptide. A spectral library was generated, which included seven peptides (four from S and three from NP) and the three to four top transitions for each and their heavy counterparts (Table S1 and Figures S2 and S3). The inclusion list contained iRT peptides, mucin SAC, and SB peptides for data alignment and digestion controls (see Tables S2 and S3). The peptides targeting S are unique to SARS-CoV-2. The NP-targeted peptide GFYAEGSR has 100% homology with SARS-CoV-1, while ADETQALPQR has 90% homology and DQVILLNK has 87.5% homology. Although these peptides/transitions showed the most robust response in our assay, there are potentially many other peptides from the

SARS-CoV-2 S and NP sequences that would be satisfactory for accurate targeting.

**PRM Assay Development.** To determine the realistic LOD and LOQ for a targeted MS analysis, the proteins of interest should be analyzed in a relevant complex biological background.<sup>17</sup> This helps to identify at an early stage of the method development, matrix effects and other interfering analytes that could potentially reduce detection of the target peptides. Therefore, we next performed a dilution series of the digested recombinant S and NP (3 amol to 12.5 fmol) with the addition of iRT peptides in a digest background containing in vitro derived mucus. Primary human bronchial epithelial cells were obtained from bronchial biopsy specimens and cultured under ALI conditions to generate in vitro derived mucus, which was used for this purpose.<sup>26</sup> We reasoned that nasal secretions may provide the best biological sample for SARS-CoV-2 virus detection and, therefore, a mucus sample would offer a relevant biological background. We also performed a “reverse” experiment in which the concentration of the isotopically labeled peptides was varied from 3 amol to 25 fmol, while the light peptide concentrations remained fixed at 12.5 fmol. The samples were subsequently analyzed by nLC-MS/MS on a Q-Exactive HF-X mass spectrometer using a 7 min separation gradient. Each dilution series was run on two separate days using three technical replicates. Using the sum of the peak areas from the four best transitions, we constructed calibration curves. PRM allows the MS/MS sequence

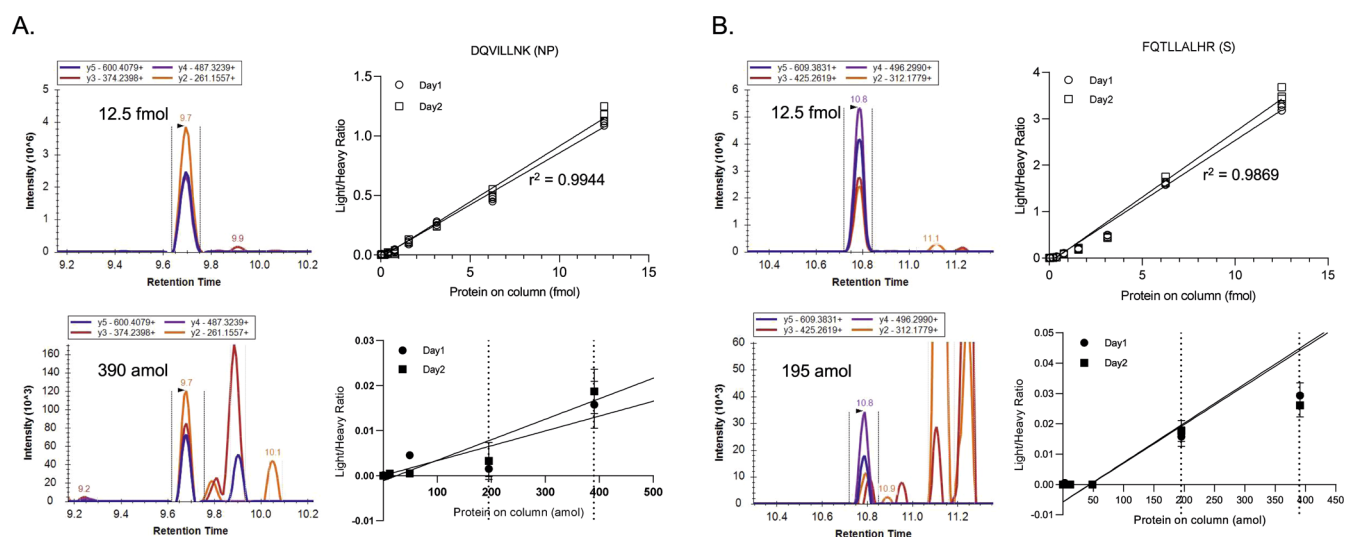


**Figure 4.** Chromatograms and calibration curves for two best target peptides used in the PRM assay for SARS CoV-2 spike protein and nucleoprotein. The summed area under curve values for the top four transitions of each peptide were taken to generate calibration curves for quantitation. The right panels display chromatograms obtained for each of transitions shown in different colors for (A) DQVILLNK (NP) and (B) FQTLALHR (S). Three technical replicates were run on two separate days. The chromatograms on the left of each panel show a low and high standard from the SARS CoV-2 S and NP in a mucin background. Calibration curves were constructed from the PRM data (top right) and zoomed in (bottom right) displaying mean values at the low end of the curve to show the LOD (left dotted line) and LOQ (right dotted line).

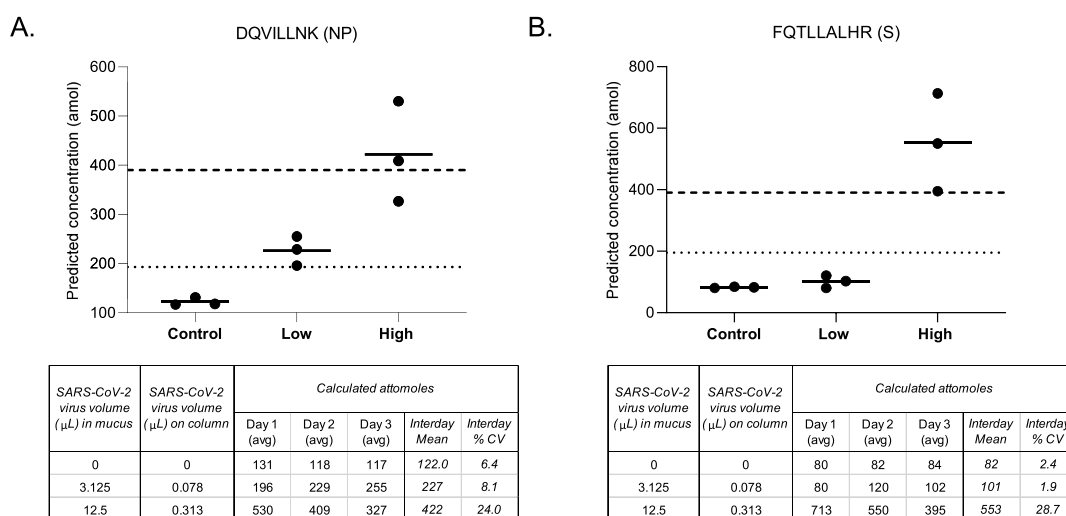


**Figure 5.** PRM assay results of mock (SARS-CoV-2 spiked) samples. Three biological replicates processed on different days and averaged from three technical replicates from each mock sample were evaluated using the calibration curves for the two best performing peptides (A) DQVILLNK and (B) FQTLALHR. The samples represent the spiked-in amounts; low (3.125  $\mu\text{L}$ ) and high (12.5  $\mu\text{L}$ ) of inactivated SARS-CoV-2 virions into in vitro derived mucus. Tables below display the average calculated amol amounts obtained on each day along with the interday mean and % CV. The dotted line indicates the calculated LOD and the dashed line indicated the LOQ determined from the calibration curves generated for each peptide.

confirmation of each peptide from the SARS-CoV-2 S-protein simultaneously while monitoring peptide/transition levels for quantitation providing high specificity. Peptides were ranked based on the linear response, precision of the calibration curves obtained on different days, and agreement between the H/L and L/H ratios as determined from the “reverse” experiment (see Table S4).

From the original spectral library, the best performing peptides for NP were (DQVILLNK: aa 348–355) and (ADETQALPQR: 376–385) and the top peptides for S were (NIDGYFK: 196–202) and (FQTLALHR: aa 238–246) (Figures S7, S10, and S11). The linear response and adjusted  $r^2$  values of the calibration curves of the selected

target peptides were between 0.995 and 0.986 over a concentration range of 3 amol to 12.5 fmol (Table 1). These four peptides also exhibited the lowest retention time shift (Figures S4–S6.). Of the poor performing peptides, GFYAEGSR gave inconsistent results especially at the low end of the calibration curve likely because of the fact that it contains a labile phosphorylated serine (see Figure S12).

To further evaluate the selected peptides as good targets for S and NP quantitation, we evaluated the missed cleavages associated with each of the four selected candidate peptides. Using the data from the dilution series, the percentage of the intensity area for the target peptide was compared with different missed cleavage forms. Although this method does

not consider ionization efficiency differences, it would allow us to evaluate a high number of potential missed cleavages, which may lower quantitation accuracy. As shown in Figure S6, there was a prominent missed cleavage peptide found for ADETQALPQR (KADETQALPQR), which accounted for almost 30% of the total intensity observed for the tryptic peptide; therefore, we eliminated this peptide as a good target for our assay. A recent report by Gouveia et al., which evaluated 101 SARS-CoV-2 peptides for targeted analysis also detected many missed cleavages around these peptides, as well as low human-virus interspecies conservation, making them a potential mutational hot-spot.<sup>27</sup> The peptide NIDGYGFK from S exhibited 18.9% of total intensity from missed cleavages and, therefore, also was not selected as a good target.

The best performing peptide targeting SARS-CoV-2 NP in a mucin background was DQVILLNK (Table 1, Figure 4A). We detected evidence of four missed cleavages for DQVILLNK, but they only accounted for 8.9% of the total intensity observed (Figure S6). This peptide provided a calibration curve with an  $r^2$  of 0.995 with LOD and LOQ values of 195 and 390 amol, respectively. FQTLALHR was the best performing peptide for S. This peptide exhibited more variability in the dilution series ( $r^2 = 0.986$ ), but the calibration curve also returned an LOD of 195 amol and LOQ of 390 amol (Table 1, Figure 4B). FQTLALHR exhibited a very low missed cleavage % signal rate (0.21%), which was confirmed in the report cited above. Interestingly, this peptide also has high intraspecies conservation.<sup>27</sup>

**Validation of PRM Assay and Feasibility of Detection for SARS-CoV-2 S and NP in Mock Viral Samples.** We next evaluated the SARS-CoV-2 PRM assay by creating a mock test sample, which contained in vitro derived mucus spiked with authentic SARS-CoV-2 virions. A stock culture supernatant of SARS-CoV-2 infected cells was inactivated using a denaturing buffer and heat. This material was spiked into the mucus samples at two different volumes to create low and high virus mock samples. A control sample containing no virus material was also evaluated. This material was digested on three separate days and run in triplicate to evaluate reproducibility of the method. Using the calibration curve from the best performing peptide for NP (DQVILLNK), the low and high SARS-CoV-2 mock samples contained on average 227 and 422 amol of NP, respectively, on column (see Figure 5A). The low virus sample result is only slightly above the LOD for this peptide of 195 amol, and the high virus sample average is above the LOQ of 390 amol. Control samples indicated a moderate level of interference, which was well below the LOQ. The level of variability observed in the low virus mock sample was acceptable over the three days (CV = 8.1%). A higher level of variability was observed between the three biological replicates in the high virus mock sample (CV = 24%). The intraday variability for this peptide was low for both the low (CV = 2.1%) and high (CV = 11.7%) mock virus samples (see Table S5).

Using the S peptide, FQTLALHR, the high virus mock sample was calculated to contain an average of 553 amol (see Figure 5B). The low virus sample results for this peptide were below the LOD of 195 amol. The high virus average value, however, was well above the LOQ of 390 amol. The interday variability between the high virus mock samples obtained over 3 days was relatively high (CV = 28.7%), but the intraday variability for this peptide was acceptable (CV = 7.9%). We suspect that the culture medium, and/or inactivation solution

in the virus material is increasing background and reducing digestion efficiency when higher amounts are spiked in.

Our results indicate that attomole sensitivity is achievable for these SARS-CoV-2 proteins in a complex background containing mucus using our PRM technique. In order to determine, if the level of sensitivity obtained in the PRM assay will be adequate to detect the presence of SARS-CoV-2 S and NP in real clinical samples, we first needed to consider the titer of the SARS-CoV-2 viral stock we used for the mock samples. After inactivation, the viral titer of the inactivated virus material was  $\sim 9.3 \times 10^6$  pfu/mL. Recent reports have indicated that the SARS-CoV-2 viral load in nasal-derived swabs ranges from  $1 \times 10^4$  to  $1 \times 10^{10}$  copies RNA/mL, while the viral titer in saliva samples ranges from  $1 \times 10^5$  to  $1 \times 10^{11}$  copies/mL as determined by RT-PCR.<sup>28</sup> Copies/mL can be compared to virus particles/mL because each virus carries one copy of the RNA sequence amplified and detected. If we consider that each of the mock samples represents a volume of original virus stock diluted in mucus in a total reaction volume of 150  $\mu$ L, we can extrapolate the representative titer for each sample. For example, the low virus sample contained 3.125  $\mu$ L of material from the original SARS-CoV-2 stock, which contained  $9.26 \times 10^6$  particles/mL. Therefore, before S-trap processing, this sample represented a titer of  $2 \times 10^5$  particles/mL in the original mucus containing sample. Likewise, the high virus sample contained  $8 \times 10^5$  particles/mL. Therefore, our PRM assay should have adequate sensitivity to detect SARS-CoV-2 in samples with a titer above  $\sim 2 \times 10^5$  particles or copies/mL. Because that is the lower range of the observed titer from saliva and nasal swab samples, this bodes well for future clinical applications for PRM-based diagnostic applications. Furthermore, viral S-protein or NP shed at the site of infection and collected in the nasal swab or mucus sample could potentially contribute to the total protein level available for detection. Finally, considering that the inactivation step, which was required for the safe handling of the viral sample in our laboratory, was not optimized for the final PRM assay, it is feasible that a PRM-based assay can deliver the level of sensitivity necessary for the detection of authentic virus at titers below  $2 \times 10^5$  copies/mL. Of the two peptides, we selected for the final assay, FQTLALHR from the spike protein is unique to SARS CoV-2, while DQVILLNK from NP shares 87.5% aa homology with SARS-CoV-1. Additional peptides could be added to the PRM assay, which are specific for SARS-CoV-1, thereby making the assay discriminatory between the two viruses.

Recent work has suggested that nLC-MS/MS over a 3 min gradient was adequate for the detection of SARS-CoV-2 peptides from nasal swabs.<sup>29</sup> While the authors did not evaluate extensively the LOD in their study, it indicates that shorter run times are possible. The PRM assay we have developed employs a processing and digestion time of approximately 4 h and a short 7 min gradient. To facilitate sample throughput, automated preparation of samples for processing and digestion could be performed in a 96-well plate format. Thus, the turnaround time for the PRM assay could match that of RT-PCR based tests. SARS-CoV-2 NP has also been detected in diluted gargle solutions from infected patients using nLC-MS/MS.<sup>30</sup> Although a 3 h gradient was needed for detection, the use of an easily collected gargle or saliva solution would be advantageous for creating a high-throughput assay.

In conclusion, the results of this proof-of-principle study indicate that a PRM assay for the quantification of SARS-CoV-2

S and NP will deliver adequate sensitivity for clinical patient samples of mucus at viral titers in the range of  $1-2 \times 10^5$ . Additionally, this assay could be used to evaluate the presence of SARS-CoV-2 in archived or recently collected biological fluids or in vitro derived research materials. The PRM assay could also be exploited to evaluate viral contamination in environmental samples, such as sewer and waste water, because of the inherent higher stability of peptides than viral RNA. Future development of the PRM assay in a saliva background may also prove useful as it would allow patients to self-collect samples and send them to reference labs for testing. Potentially, MS-based methods could serve as a complementary diagnostic tool to RT-PCR and may deliver a higher throughput with increased safety because the virus can be fully deactivated at the site of collection without sacrificing the ability to detect antigens. Considering the current slow pace of RT-PCR testing for SARS-CoV-2 and the difficulty in obtaining RNA extraction materials and PCR primers, antigen detection methods should be explored for the development of rapid point-of-care assays. Therefore, studies that estimate viral protein antigen levels in clinically relevant samples such as this also have value in ascertaining if rapid test paradigms such as lateral flow immuno-assays would have adequate sensitivity for SARS-CoV-2 infection diagnosis.

## ■ ASSOCIATED CONTENT

### SI Supporting Information

The Supporting Information is available free of charge at <https://pubs.acs.org/doi/10.1021/acs.analchem.0c02288>.

MS raw data and associated skyline analysis (PDF)

## ■ AUTHOR INFORMATION

### Corresponding Author

**Sonja Hess** – *Dynamic Omics, Antibody Discovery and Protein Engineering (ADPE), R&D AstraZeneca, Gaithersburg 20878, Maryland, United States*; Email: [Sonja.Hess@AstraZeneca.com](mailto:Sonja.Hess@AstraZeneca.com)

### Authors

**Lisa H. Cazares** – *Dynamic Omics, Antibody Discovery and Protein Engineering (ADPE), R&D AstraZeneca, Gaithersburg 20878, Maryland, United States*; [orcid.org/0000-0001-5754-6192](https://orcid.org/0000-0001-5754-6192)

**Raghothama Chaerkady** – *Dynamic Omics, Antibody Discovery and Protein Engineering (ADPE), R&D AstraZeneca, Gaithersburg 20878, Maryland, United States*

**Shao Huan Samuel Weng** – *Dynamic Omics, Antibody Discovery and Protein Engineering (ADPE), R&D AstraZeneca, Gaithersburg 20878, Maryland, United States*

**Chelsea C. Boo** – *Dynamic Omics, Antibody Discovery and Protein Engineering (ADPE), R&D AstraZeneca, Gaithersburg 20878, Maryland, United States*

**Raffaello Cimbri** – *Dynamic Omics, Antibody Discovery and Protein Engineering (ADPE), R&D AstraZeneca, Gaithersburg 20878, Maryland, United States*

**Hsiang-En Hsu** – *Dynamic Omics, Antibody Discovery and Protein Engineering (ADPE), R&D AstraZeneca, Gaithersburg 20878, Maryland, United States*

**Sarav Rajan** – *Biological Therapeutics 1, Antibody Discovery and Protein Engineering (ADPE), R&D AstraZeneca, Gaithersburg 20878, Maryland, United States*

**William Dall'Acqua** – *Biological Therapeutics 1, Antibody Discovery and Protein Engineering (ADPE), R&D AstraZeneca, Gaithersburg 20878, Maryland, United States*

**Lori Clarke** – *Cell Therapeutics, Antibody Discovery and Protein Engineering (ADPE), R&D AstraZeneca, Gaithersburg 20878, Maryland, United States*

**Kuishu Ren** – *Discovery Anti Infection, Microbial Sciences, R&D AstraZeneca, Gaithersburg 20878, Maryland, United States*

**Patrick McTamney** – *Discovery Anti Infection, Microbial Sciences, R&D AstraZeneca, Gaithersburg 20878, Maryland, United States*

**Nicole Kallewaard-LeLay** – *Discovery Anti Infection, Microbial Sciences, R&D AstraZeneca, Gaithersburg 20878, Maryland, United States*

**Mahboobe Ghaedi** – *Respiratory and Immunology, R&D AstraZeneca, Gaithersburg 20878, Maryland, United States*

**Yasuhiro Ikeda** – *Cell Therapeutics, Antibody Discovery and Protein Engineering (ADPE), R&D AstraZeneca, Gaithersburg 20878, Maryland, United States*

Complete contact information is available at:

<https://pubs.acs.org/10.1021/acs.analchem.0c02288>

### Author Contributions

The manuscript was written through contributions of all authors. All authors have given approval to the final version of the manuscript.

### Notes

The authors declare no competing financial interest.

## ■ ACKNOWLEDGMENTS

We thank Travis Warren [Integrated Research Facility at Fort Detrick (IRF)—Frederick] for facilitating the SARS-CoV-2 virus transfer and Herren Wu for support.

## ■ REFERENCES

- (1) Mackay, I. M.; Arden, K. E. *Virology* **2015**, *12*, 222.
- (2) Wang, W.; Xu, Y.; Gao, R.; Lu, R.; Han, K.; Wu, G.; Tan, W. *JAMA* **2020**, *323*, 1843–1844.
- (3) Huang, C.; Wang, Y.; Li, X.; Ren, L.; Zhao, J.; Hu, Y.; Zhang, L.; Fan, G.; Xu, J.; Gu, X.; Cheng, Z.; Yu, T.; Xia, J.; Wei, Y.; Wu, W.; Xie, X.; Yin, W.; Li, H.; Liu, M.; Xiao, Y.; Gao, H.; Guo, L.; Xie, J.; Wang, G.; Jiang, R.; Gao, Z.; Jin, Q.; Wang, J.; Cao, B. *Lancet* **2020**, *395*, 497–506.
- (4) Zhao, J.; Yuan, Q.; Wang, H.; Liu, W.; Liao, X.; Su, Y.; Wang, X.; Yuan, J.; Li, T.; Li, J.; Qian, S.; Hong, C.; Wang, F.; Liu, Y.; Wang, Z.; He, Q.; Li, Z.; He, B.; Zhang, T.; Fu, Y.; Ge, S.; Liu, L.; Zhang, J.; Xia, N.; Zhang, Z. *Clin. Infect. Dis.* **2020**, *ciaa344*.
- (5) Zhang, N.; Wang, L.; Deng, X.; Liang, R.; Su, M.; He, C.; Hu, L.; Su, Y.; Ren, J.; Yu, F.; Du, L.; Jiang, S. *J. Med. Virol.* **2020**, *92*, 408–417.
- (6) Li, F. *Annu. Rev. Virol.* **2016**, *3*, 237–261.
- (7) Lesur, A.; Doman, B. *Proteomics* **2015**, *15*, 880–890.
- (8) Boja, E. S.; Rodriguez, H. *Proteomics* **2012**, *12*, 1093–1110.
- (9) Huttenhain, R.; Soste, M.; Selevsek, N.; Rost, H.; Sethi, A.; Carapito, C.; Farrah, T.; Deutsch, E. W.; Kusebauch, U.; Moritz, R. L.; Nimeus-Malmstrom, E.; Rinner, O.; Aebersold, R. *Sci. Transl. Med.* **2012**, *4*, 142ra94.
- (10) Cho, W. C. *Expert Rev. Proteomics* **2017**, *14*, 725–727.
- (11) Pechlaner, R.; Tsimikas, S.; Yin, X.; Willeit, P.; Baig, F.; Santer, P.; Oberhollenzer, F.; Egger, G.; Witztum, J. L.; Alexander, V. J.; Willeit, J.; Kiechl, S.; Mayr, M. *J. Am. Coll. Cardiol.* **2017**, *69*, 789–800.
- (12) Li, S.; Nakayama, T.; Akinc, A.; Wu, S.-L.; Karger, B. L. *J. Pharmacol. Toxicol. Methods* **2015**, *71*, 110–119.



- (13) Wee, S.; Alli-Shaik, A.; Kek, R.; Swa, H. L. F.; Tien, W.-P.; Lim, V. W.; Leo, Y.-S.; Ng, L.-C.; Hapuarachchi, H. C.; Gunaratne, J. *Proc. Natl. Acad. Sci. U.S.A.* **2019**, *116*, 6754–6759.
- (14) Ward, M. D.; Kenny, T.; Bruggeman, E.; Kane, C. D.; Morrell, C. L.; Kane, M. M.; Bixler, S.; Grady, S. L.; Quizon, R. S.; Astatke, M.; Cazares, L. H. *Clin. Proteomics* **2020**, *17*, 11.
- (15) Wrapp, D.; Wang, N.; Corbett, K. S.; Goldsmith, J. A.; Hsieh, C.-L.; Abiona, O.; Graham, B. S.; McLellan, J. S. *Science* **2020**, *367*, 1260–1263.
- (16) HaileMariam, M.; Eguez, R. V.; Singh, H.; Bekele, S.; Ameni, G.; Pieper, R.; Yu, Y. *J. Proteome Res.* **2018**, *17*, 2917–2924.
- (17) Moradian, A.; Porras-Yakushi, T. R.; Sweredoski, M. J.; Hess, S. *Methods Mol. Biol.* **2016**, *1394*, 75–85.
- (18) Escher, C.; Reiter, L.; MacLean, B.; Ossola, R.; Herzog, F.; Chilton, J.; MacCoss, M. J.; Rinner, O. *Proteomics* **2012**, *12*, 1111–1121.
- (19) Gallien, S.; Duriez, E.; Crone, C.; Kellmann, M.; Moehring, T.; Domon, B. *Mol. Cell. Proteomics* **2012**, *11*, 1709–1723.
- (20) Egerton, J. D.; Kuehn, A.; Merrihew, G. E.; Bateman, N. W.; MacLean, B. X.; Ting, Y. S.; Canterbury, J. D.; Marsh, D. M.; Kellmann, M.; Zabrouskov, V.; Wu, C. C.; MacCoss, M. J. *Nat. Methods* **2013**, *10*, 744–746.
- (21) Zahn-Zabal, M.; Michel, P. A.; Gateau, A.; Nikitin, F.; Schaeffer, M.; Audot, E.; Gaudet, P.; Duek, P. D.; Teixeira, D.; Rech de Laval, V.; Samarasinghe, K.; Bairoch, A.; Lane, L. *Nucleic Acids Res.* **2020**, *48*, D328–D334.
- (22) Azadeh, M.; Gorovits, B.; Kamerud, J.; MacMannis, S.; Safavi, A.; Sailstad, J.; Sondag, P. *AAPS J.* **2018**, *20*, 22.
- (23) Honour, J. W. *Ann. Clin. Biochem.* **2011**, *48*, 97–111.
- (24) Watanabe, Y.; Allen, J. D.; Wrapp, D.; McLellan, J. S.; Crispin, M. *Science* **2020**, *369* (6501), 330–333.
- (25) Davidson, A. D.; Williamson, M. K.; Lewis, S.; Shoemark, D.; Carroll, M. W.; Heesom, K. J.; Zambon, M.; Ellis, J.; Lewis, P. A.; Hiscox, J. A.; Matthews, D. A. *Genome Med.* **2020**, *12*, 68.
- (26) Abdullah, L. H.; Wolber, C.; Kesimer, M.; Sheehan, J. K.; Davis, C. W. *Methods Mol. Biol.* **2012**, *842*, 259–277.
- (27) Gouveia, D.; Grenga, L.; Gaillard, J. C.; Gallais, F.; Bellanger, L.; Pible, O.; Armengaud, J. *Proteomics* **2020**, *20*, 2000107.
- (28) To, K. K.-W.; Tsang, O. T.-Y.; Leung, W.-S.; Tam, A. R.; Wu, T.-C.; Lung, D. C.; Yip, C. C.-Y.; Cai, J. P.; Chan, J. M.-C.; Chik, T. S.-H.; Lau, D. P.-L.; Choi, C. Y.-C.; Chen, L.-L.; Chan, W.-M.; Chan, K.-H.; Ip, J. D.; Ng, A. C.-K.; Poon, R. W.-S.; Luo, C.-T.; Cheng, V. C.-C.; Chan, J. F.-W.; Hung, I. F.-N.; Chen, Z.; Chen, H.; Yuen, K.-Y. *Lancet Infect. Dis.* **2020**, *20*, 565–574.
- (29) Gouveia, D.; Miotello, G.; Gallais, F.; Gaillard, J.-C.; Debroas, S.; Bellanger, L.; Lavigne, J.-P.; Sotto, A.; Grenga, L.; Pible, O.; Armengaud, J. *J. Proteome Res.* **2020**, DOI: 10.1021/acs.jproteome.0c00535.
- (30) Ihling, C.; Tänzler, D.; Hagemann, S.; Kehlen, A.; Hüttelmaier, S.; Arlt, C.; Sinz, A. *J. Proteome Res.* **2020**, DOI: 10.1021/acs.jproteome.0c00280.